Performance Evaluation of Poly 3-(Phenylthiophene) Derivatives as Active Materials for Electrochemical Capacitor Applications

J. P. Ferraris,* M. M. Eissa, I. D. Brotherston, and D. C. Loveday

Department of Chemistry, University of Texas at Dallas, P.O. Box 830688, Richardson, Texas 75083-0688

Received April 27, 1998. Revised Manuscript Received July 16, 1998

Electroactive polymers from 3-(4-fluorophenyl)thiophene, 3-(4-cyanophenyl)thiophene, 3-(4-methylsulfonylphenyl)thiophene, and 3-(3,4-difluorophenyl)thiophene were electrochemically deposited onto carbon paper electrodes from tetramethylammonium trifluoromethanesulfonate ($Me_4NCF_3SO_3$)/acetonitrile and/or tetraethylammonium tetrafluoroborate (Et_4NBF_4)/acetonitrile electrolyte solutions. The morphologies and electrochemical performance of the films were shown to depend on both the growth and cycling electrolytes. Constant current multicycle tests were performed on model single-cell devices using the type III capacitor configuration at high voltage (2.8−2.9 V). Active material energy and power densities of up to 50 Wh/kg and 5 kW/kg were achieved at discharge rates of 50 and 10 mA/cm^2, respectively. The long-term stabilities (up to 1000 cycles) of these polymers were investigated by repeated charging and discharging using cyclic voltammetry in both the p- and n-doping regimes.

Introduction

Increased performance requirements for electric vehicles (EV) have created the need for a reliable secondary source to provide peak power. Although the use of extra batteries has been considered, modern batteries are generally incapable of producing the required peak currents without degradation of their long-term performance. Furthermore, new battery technologies may be still too expensive to be commercially viable today.[1,2]

One approach to meeting the criteria required of the energy storage system in the EV is the use of a hybrid source consisting of a pulse power unit to provide the peak power and a battery to provide the energy to maintain the vehicle's momentum. Electrochemical capacitors (ECCs) can provide high power for acceleration and hill-climbing. Unlike most galvanic cells or batteries, but similar to electrostatic capacitors, these systems can be rapidly and repeatedly cycled through their charging/discharging process. These devices therefore fill the void between batteries and conventional capacitors in terms of their energy and power densities and are thus ideally suited for the load-leveling required in an EV.[1,3−8]

Other applications for ECCs include power sources for the space industry, airplane wing deicing, industrial robotics and arc welding, home appliances, and compact power devices for cordless telephones and electronic toys. Market growth depends on improvements in materials and achieving the performance targets required by consumers. Some of the remaining challenges include the development of multilayer stacks, reduction in weight and cost, and the ability to mass-produce with quality.[9,10]

Two families of electrochemical capacitors, with different modes of energy storage, are currently being developed. The first are devices based on the double-layer capacitance of the particle/solution interface at high surface area electrode materials (e.g., carbon) where the capacitance is electrostatic in origin. High-performance devices of this type are already on the market.[5,9,11−14] The second are redox electrochemical capacitors using metal oxides such as RuO_2[7,15,16] and

(1) Burke, A. F. Electrochemical Capacitors for Electric Vehicles—Technology Update and Implementation Considerations. 12th International Electric Vehicle Symposium (EVS-12), October 1994.
(2) Burke, A. F.; Murphy, T. C. Material Characteristics and the Performance of Electrochemical Capacitors for Electric/Hybrid Vehicles. Materials Research Society Spring Meeting, April 1995.
(3) Andrieu, X.; Crepy, G.; Josset, L. Supercapacitor Based on Liquid Organic and Polymer Electrolytes for Electric Vehicles. Third International Seminar on Double Layer Capacitors and Similar Energy Storage Devices, Deerfield Beach, FL, December 6−8, 1993.
(4) Conway, B. E.; Gileadi, E. *Trans. Faraday Soc.* **1962**, *58*, 2493.
(5) Conway, B. E. Some Basic Electrochemical Principles Involved in Supercapacitor Operation and Development. Third International Seminar on Double Layer Capacitors and Similar Energy Storage Devices, Deerfield Beach, FL, December 6−8, 1993.
(6) Conway, B. E., *J. Electrochem. Soc.* **1991**, *138* (6), 1539.
(7) Raistrick, I. D. In *The Electrochemistry of Semiconductors and Electronics, Processes and Devices*; McHardy, J., Ludwig, F., Eds.; Noyes: New Jersey, 1992; p 297.
(8) Rudge, A.; Davey, J.; Raistrick, I.; Gottesfeld, S.; Ferraris, J. P. *J. Power Sources* **1994**, *47*, 89.
(9) Nishino, A. *J. Power Sources* **1996**, *60*, 137.
(10) Finello, D. New Developments in Ultracapacitor Technology. Fourth International Seminar on Double Layer Capacitors and Similar Energy Storage Devices, Deerfield Beach, FL, December 12−14, 1994.
(11) Mayer, S. T.; Pekala, R. W.; Kaschrnittcr, J. L. *J. Electrochem. Soc.* **1993**, *140*, 446.
(12) Conway, B. E. Design and Evaluation of Capacitor Energy Storage Devices. Third International Seminar on Double Layer Capacitors and Similar Energy Storage Devices, Deerfield Beach, FL, December 6−8, 1993.
(13) Matsuda, Y.; Morita, M.; Ishikawa M.; Ihara, M. *J. Electrochem. Soc.* **1993**, *140*, L109.
(14) McEwen, A. B.; Chadha, R.; Blakley, T.; Koch, V. $EMIPF_6$ Based Nonaqueous Electrolytes For Electrochemical Capacitors. Electrochemical Society Proceedings, 1996; Vol. 96-25, p 313.

10.1021/cm9803105 CCC: $15.00
Published on Web 10/09/1998

conducting polymers.[17−23] In these systems electrons are transferred in to and out of three-dimensional materials while ion transfer occurs across the electrode/electrolyte interface. ECCs based on this mechanism have higher energy densities than double-layer capacitors. Conducting polymers have the added advantage that they are considerably less expensive than RuO_2.[18]

Conducting polymers have been employed as the cathode materials in Li-ion batteries[24−30] and as the electroactive materials for both electrodes in electrochemical capacitors.[8,31−35] ECCs based on conducting polymers store their charge in a similar way to Li-ion batteries in that they utilize ion insertion/extraction as the charge storage process.

Most conducting polymers can be p-doped reversibly and this process generally takes place at electrode potentials that are accessible in aqueous solutions. Conversely, only a limited number of conducting polymers, including polyacetylene,[28,36,37] poly-*p*-phenylene,[30] and polythiophene and its derivatives,[38−41] can be reversibly n-doped, all at highly reducing electrode potentials that requires cathodically stable and relatively pure nonaqueous systems.

Conducting polymers can be prepared either chemically or electrochemically, and in the majority of cases this is done by oxidation of the relevant monomer in solution. When p-doped electrochemically, electrons are removed from the polymer backbone through the external circuit and anions from the electrolyte solution are incorporated into the polymer film to counterbalance the positive charge. In this state, the polymer has high electronic conductivity. The n-doping process proceeds with the injection of electrons onto the polymer backbone by the external circuit, while cations enter the polymer from the solution phase in order to maintain overall charge neutrality.[8,32] Both doping processes are facilitated by high ionic conductivities and this requirement can be fulfilled by producing a material that has a network of electrolyte-filled pores. Of some concern are the high negative potentials required for the n-doping process. This makes the polymer susceptible to attack by reactive species in the electrolyte solution, which can reduce the cycle life. Overcoming this limitation is vital if practical ECCs based on conducting polymers are to be realized.

The available stored energy for an ECC is determined by the quantity of the electroactive materials, their standard electrode potentials, and their total reversible charge. The electrolyte in an ECC should have a high breakdown voltage for greater energy storage (energy $= \int V \, dQ$) and low ionic resistance for greater power. Despite their lower ionic conductivities[42,43] organic electrolytes have received considerable attention[18] due to their greater electrochemical stability (>3 V) compared to aqueous systems (∼1 V).

We have previously described three schemes (I−III) by which conducting polymers can be applied as the active material in electrochemical capacitors.[8,31] The types I and II capacitors are symmetric and asymmetric devices, respectively, which utilize p-dopable conducting polymers such as polyaniline (PAni),[18] polypyrrole (PPy),[18,44] and polythiophene.[8,34] However, reliance on p-doping/dedoping alone typically limits the overall voltage of the device to about 1 V in the type I configuration and 1.5 V in the type II configuration. In the type III configuration, a conducting polymer that is both p- and n-dopable is used to create a symmetrical ECC. The greater voltage (∼3 V) and high electronic conductivity in the charged device leads to improved energy and power densities. An additional feature of the type III configuration is its relatively flat discharge profile in which the device voltage does not fall steadily during discharge but remains relatively constant until the maximum level of discharge is reached.

Derivatization of 3-phenylthiophene monomers with electron-withdrawing groups on the phenyl rings has been shown to enhance the stability of the n-doped polymer when counterions such as tetraalkylammonium cations are employed.[8,45,46] We recently reported the synthesis, polymerization potential, stability, ionic re-

(15) Miller, J. R. Performance of Mixed Metal Oxide Pseudocapacitors: Comparison with Carbon Double Layer Capacitors. Second International Seminar on Double Layer Capacitors and Similar Energy Storage Devices, Deerfield Beach, FL, December 7−9, 1992.
(16) Zheng, J. P.; Cygan, P. G.; Jow, T. R. *J. Electrochem. Soc.* **1995**, *142*, 2699.
(17) Yata, S.; Okamoto, E.; Satake, H.; Kubota, H.; Fujii, M.; Taguchi, T.; Kinoshita, H. *J. Power Sources* **1996**, *60*, 207.
(18) Rudge, A.; Davey, J.; Uribe, F.; Landeros, J., Jr.; Gottesfeld, S. Performance Evaluation of Polypyrrole and Polyaniline as Active Materials for Electrochemical Capacitors. Third International Seminar on Double Layer Capacitors and Similar Energy Storage Devices, Deerfield Beach, FL, December 6−8, 1993.
(19) Novak, P.; Muller, K.; Santhanam, K.; Haas, O. *Chem. Rev.* **1997**, *97*, 207.
(20) Naoi, K.; Oura, Y.; Tsuimoto, H. Dual Mode Ion Switching Conducting Polymer Film as a High Energy Supercapacitor Material. Electrochemical Society Proceedings 1995, Vol. 95-29, p 162.
(21) Huang, S. C.; Huang, S. M.; Ng, H.; Kaner, R. B. *Synth. Met.* **1993**, *55−57*, 4047.
(22) Sarker, H.; Gofer, Y.; Killian, J. G.; Poehler, T. O.; Searson, P. C. *Synth. Met.* **1997**, *88*, 179.
(23) Satoh, M.; Ishikawa, H.; Amano, K.; Hasegawa E.; Yoshino, K. *Synth. Met.* **1995**, *71*, 2259.
(24) Panero, S.; Spila, E.; Scrosati, B. *J. Electrochem. Soc.* **1996**, *143*, L29.
(25) Shacklette, L.; Elsenbaumer, R.; Chance, R.; Sowa, J.; Ivory, D.; Miller G.; Baughman, R. *J. Chem. Soc., Chem. Commun.* **1982**, 361.
(26) Koga, K.; Yamasaki, S.; Narimatsu, K.; Takayangi, M. *Polym. J.* **1989**, *21* (9), 733.
(27) Kaufman, J. H.; Chung, T. C.; Heeger, A. J.; Wudl, F. *J. Electrochem. Soc.* **1984**, *131*, 2092.
(28) MacInnes, D.; Druy, M.; Nigrey, P.; Nairns, D.; MacDiarmid, A.; Heeger, A. *J. Chem. Soc., Chem. Commun.* **1981**, 317.
(29) Moon, D.; Padias, A.; Hall, J. K. *Macromolecules* **1995**, *28*, 6205.
(30) Shakuda, S.; Kawai, T.; Morita, S.; Yoshino, K. *Jpn. J. Appl. Phys.* **1994**, *33* (1), 4121.
(31) Rudge, A.; Davey, J.; Raistrick, I.; Gottesfeld S.; Ferraris, J. P. *Electrochim. Acta* **1994**, *39*, 273.
(32) Ren, X.; Gottesfeld, S.; Ferraris, J. P. *Proc. Electrochem. Soc.* **1995**, *95-29*, 138.
(33) Mastragostino, M.; Arbizzani, C.; Cerroni, M. G.; Paraventi, R. *Proc. Electrochem. Soc.* **1996**, *96-25*, 109.
(34) Arbizzani, C.; Mastragostino, M.; Meneghello, L. *Electrochim. Acta* **1996**, *41*, 21.
(35) Arbizzani, C.; Catellani, M.; Mastragostino M.; Mingazzini, C. *Electrochim Acta* **1995**, *40*, 1871.
(36) Rakovic, D. *Material Science Forum*; Trans Tech Publications: Aedermannsdorf, Switzerland, 1996; Vol. 214, p 139.
(37) Gau, S.; Milliken, J.; Pron, A.; MacDiarmid, A.; Heeger, A. *J. Chem. Soc., Chem. Commun.* **1979**, 662.
(38) Roncali, J. *Chem. Rev.* **1992**, *92*, 711.
(39) Roncali, J. *Chem. Rev.* **1997**, *97*, 173.
(40) King, G.; Higgins, S. *J. Mater. Chem.* **1995**, *5* (3), 447.
(41) Dale, S.; Glidle, A.; Hillman, R. *J. Mater. Chem.* **1992**, *2* (1), 99.
(42) Preechatiwong, W.; Schultz, J. *Polymer* **1996**, *37* (23), 5109.
(43) Ue, M.; Ida, K.; Mori, S. *J. Electrochem. Soc.* **1994**, *141* (11), 2989.
(44) Arbizzani, C.; Mastragostino, M.; Meneghello, L. Performance of Polymer-Based Supercapacitors. *Mater. Res. Soc. Symp. Proc.* **1995**, *369*, 605.
(45) Guerrero, D.; Ren, X.; Ferraris, J. P. *Chem. Mater.* **1994**, *6*, 7.

Table 1. Near-Term and Future Goals for the DOE Electrochemical Capacitor Development Programs

required properties (packaged devices)	near term	future
energy density (Wh/kg)	>5	>15
power density (kW/kg)	50	80
energy storage (Wh)	500	750
weight (kg)	<100	<50

sistance, and charge capacity of a series of new conducting polymers that can be reversibly p- and n-doped to high charge density. These polymers were obtained from 3-(4-cyanophenyl)thiophene, 3-(3,4-difluorophenyl)thiophene, 3-(3,5-difluorophenyl)thiophene, 3-(3-fluorophenyl)thiophene, and 3-(4-methylsulfonylphenyl)-thiophene.[46] We were also able to correlate the film characteristics with polymer growth conditions for each monomer. Degradation could be minimized by selecting a nonnucleophilic solvent (acetonitrile) and a suitable electrolyte salt, the most promising of which were tetramethylammonium trifluoromethanesulfonate ($Me_4NCF_3SO_3$) and tetraethylammonium tetrafluoroborate (Et_4NBF_4).

U.S. Department of Energy (DOE) targets for specific energy and peak specific power for packaged ECCs in EV applications are shown in Table 1.[47] Of particular concern for conducting polymer-based electrochemical capacitor applications is the total cycle life, which must exceed 10^5 cycles.

We describe in this paper the testing of several conducting polymers in model electrochemical capacitor configurations and the determination of the stability of these materials to repeated charge/discharge cycles. We also show that the electrical properties and morphologies of the polymer films are dependent on the nature of the anion used during the electrochemical polymerization.

Experimental Section

The monomers, 3-(4-fluorophenyl)thiophene (PFPT), 3-(3,4-difluorophenyl)thiophene (MPFPT), 3-(4-cyanophenyl)thiophene (PCNPT), and 3-(4-methylsulfonylphenyl)thiophene (PMSPT), were prepared as previously described with yields ranging from 60% to 70%.[46] All were white solids that were typically purified by sublimation and displayed satisfactory melting points and spectroscopic properties.

Tetraethylammonium tetrafluoroborate (Et_4NBF_4, Fluka) was recrystallized three times from methanol and dried under vacuum at 140 °C for 24 h before use. Tetramethylammonium trifluoromethanesulfonate ($Me_4NCF_3SO_3$) was recrystallized three times from acetone after being treated with charcoal and dried under vacuum at 180 °C for 24 h before use. Acetonitrile (Aldrich Sure-seal, <50 ppm H_2O), which was used throughout the experiments, was passed through an activated alumina column in the glovebox before use. Water content in the electrolyte solutions was determined to be <10 ppm using an Aquatest IV Karl Fisher titrator. Cyclic voltammetry was performed using a PARC model 273 potentiostat, and the data were recorded and analyzed utilizing Model 270/250 Research Electrochemistry software (version 4.0, EG&G Instruments Inc.). All polymerization, single-electrode cyclic voltammetry, and charge/discharge experiments were performed in a helium- or nitrogen-filled glovebox. All polymer films were grown in a cell containing three electrodes. The working electrode was either Pt (0.017 cm^2) or C (1 cm^2) and the counter electrode was porous carbon paper. The nonaqueous Ag/Ag^+ reference electrode was composed of a silver wire immersed in the respective working solution, with silver nitrate added at a concentration of 0.01 mol/dm^3. The formal measured potential of the ferrocene/ferrocenium (50 mM ferrocene in 0.2 M appropriate supporting electrolyte) couple was 0.085 V vs this reference electrode.

Porous, low-density carbon paper (Spectracorp, 6 μm fibers) was chosen as a support to allow high mass deposition of polymer per unit geometric area. The working and counter electrodes have thickness of 0.55 mm ($\rho = 0.22$ g/cm^3) and 1.6 mm ($\rho = 0.5$ g/cm^3), respectively. Carbon electrodes were masked with poly(vinyl chloride) (PVC) [deposited from tetrahydrofuran (THF) solution] to allow only 1 cm^2 to be accessible for polymer growth.

Electrochemical polymerizations onto the carbon papers were performed at room temperature by chronopotentiometry of acetonitrile solutions containing 0.2 M electrolyte and 0.1 M relevant monomer. Polymers from PFPT and MPFPT were deposited to a total charge of 12 C at 3 mA/cm^2 current density, whereas PCNPT and PMSPT-based polymers were deposited to a total charge of 10 C using the same current density. Such deposition charges are expected to yield polymer-coated electrodes than can provide a maximum charge of approximately 1−1.3 C given the previously determined polymerization efficiency (∼ 65−70%) and doping level (∼ 35%).[46]

Small scale type III model devices were assembled from two identical polymer-coated carbon paper electrodes, held 2−3 mm apart without a separator in a custom-built holder.

During capacitor charge/discharge cycles, a reference electrode was employed to monitor the respective electrode potentials. The electrochemical capacitor assembly was immersed in acetonitrile solutions containing either Et_4NBF_4 or $Me_4NCF_3SO_3$ (0.2 or 1.0 M) for the performance tests. An Arbin battery testing system (HSP-2043, Arbin Instruments) was used to evaluate the ECCs.

The mass of undoped polymer was obtained by weighing the electrode after removing dopant anions potentiostatically, followed by washing with acetonitrile and drying. All calculations, such as current and charge densities, are quoted per square centimeter areal dimension of carbon paper, rather than the actual carbon surface area. *Energy and power densities are calculated on the basis of the weight of the electroactive polymer only*. Before construction of the capacitor assemblies, the polymer-coated electrodes were analyzed by cyclic voltammetry using a conventional three-electrode cell arrangement.

Polymer morphologies were observed on gold-sputtered samples using a Phillips XL-30 scanning electron microscope.

We followed the procedures proposed by J. R. Miller to characterize capacitors under development for EV applications.[48] Figure 1 shows a typical charge/discharge curve for our electrochemical capacitors operated at constant current. The cell voltage increases during the charging cycle until it reaches the specified value (e.g., 2.8 V). Upon discharging, the cell voltage decreases more rapidly due to the increased current (here 10 mA/cm^2) compared to that used during charging (2 mA/cm^2).

A range of currents was selected to restrict the discharge times to less than 100 s, which is suitable for the envisaged applications. The voltage was held for 10 s at the end of each charge and discharge test cycle to establish a constant voltage level for all the tests. Five to 10 consecutive charge/discharge cycles at a specified current density were performed for each single test. The reported data are the average of the second to the fifth cycles.

(46) Eissa, M. M.; Moxey, A.; Brotherston, I. D.; Loveday, D. C.; Ferraris, J. P. *J. Electroanal. Chem.*, 1998, in press.

(47) Burke, A. F. Testing of Ultracapacitors for Electric Vehicle Applications. Third International Seminar on Double Layer Capacitors and Similar Energy Storage Devices, Deerfield Beach, FL, December 6−8, 1993.

(48) Miller, J. R.; Burke, A. F. Electric Vehicle Capacitor Test Procedures Manual Revision 0. Idaho National Engineering Laboratory, DOE/ID-10491, October 1994.

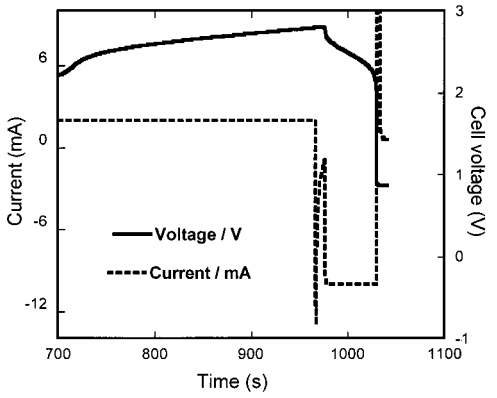

Figure 1. Typical cell voltage vs time curve for an ECC when charged to 2.8 V at 2 mA/cm^2 and discharged to 1.0 V at 10 mA/cm^2.

Table 2. Monomers, Acronyms, and Onset Oxidation Potentials

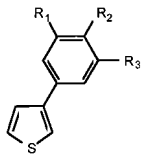

substituent R	acronym for monomer	monomer[a] $E_{oxidaton}$
R_1, R_3 = H; R_2 = F	PFPT	1.1
R_1, R_3 = H; R_2 = SO_2Me	PMSPT	1.17
R_1 = H; R_2, R_3 = F	MPFPT	1.19
R_1, R_3 = H; R_2 = CN	PCNPT	1.3

[a] Oxidation potentials were quoted vs Ag/Ag^+.

Results and Discussion

The enhancement of the ion diffusivity, which is often the rate-determining step of the charge insertion/extraction process of conducting polymer films, is critical in obtaining the high energy and power densities desired for a commercial electrochemical capacitor. We have focused on producing films with open rigid structures as we believe this morphology is conducive to high ion diffusion.[46]

Improving the n-doping properties for thicker films is another major objective for type III electrochemical capacitors. Our approaches to achieve this goal have included the design and synthesis of new monomers possessing electron-withdrawing groups and the optimization of growth and cycling conditions. The arylthiophene derivatives studied here are listed along with their acronyms in Table 2.

Effects of Growth Electrolyte on Charge/Discharge Performance. Polymer films of PFPT and MPFPT were grown from acetonitrile solutions of 0.1 M monomer in 0.2 M Et_4NBF_4 and 0.2 M $Me_4NCF_3SO_3$, respectively, and their morphologies were observed with scanning electron microscopy. Figure 2 shows the SEM image of the carbon substrates. This micrograph shows that the porosity of the carbon paper permits good access of the electrolyte solution.[8,31,32]

Figures 3−6 show the SEMs of the films from PFPT and MPFPT grown from both electrolytes onto the carbon paper substrates. The morphology of the PFPT film grown from $Me_4NCF_3SO_3$ is different from that of the film grown from Et_4NBF_4. For the latter electrolyte, the PFPT polymer is formed in relatively compact sheaths around the carbon fibers (Figure 3). This is to be contrasted with the film grown from $Me_4NCF_3SO_3$, which appears more porous and is decorated with small polymer nodules some 2−5 μm in diameter (Figure 4). Since the ionic conductivities of the two electrolytes are essentially equal at the concentrations used, it appears that the anion size can influence the structure of the polymer formed during the polymerization, with larger anions producing a material with larger pore size. *This*

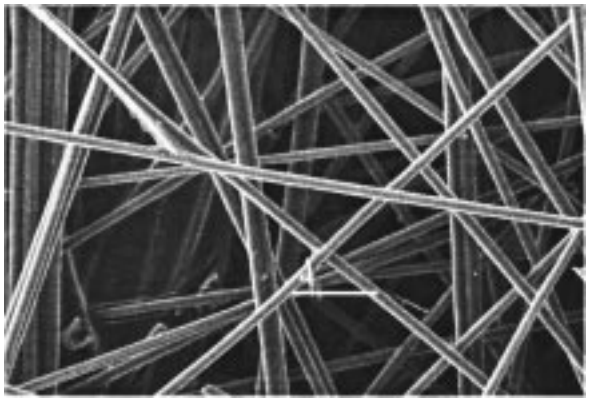

Figure 2. Scanning electron micrograph, viewed from the top surface, of the bare carbon paper electrode (bar = 50 μm).

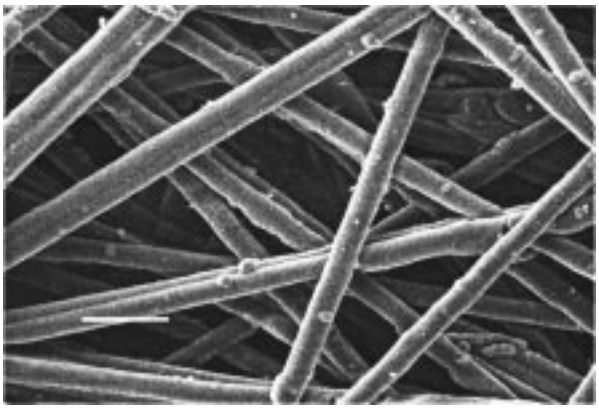

Figure 3. Scanning electron micrograph of the top surface view of a carbon paper electrode after PFPT was electrodeposited from 0.2 M Et_4NBF_4 in acetonitrile solution (bar = 50 μm).

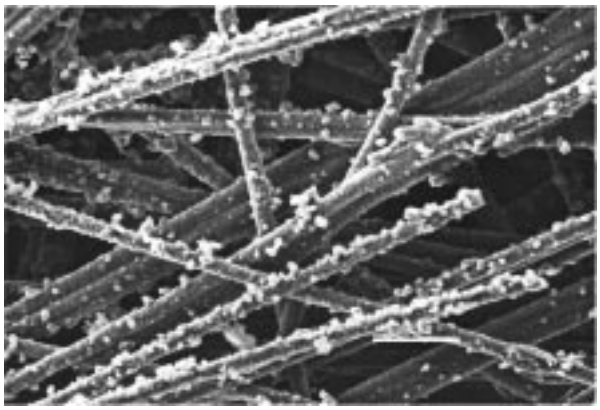

Figure 4. Scanning electron micrograph of the top surface view of a carbon paper electrode after PFPT was electrodeposited from 0.2 M $Me_4NCF_3SO_3$ in acetonitrile solution (bar = 50 μm).

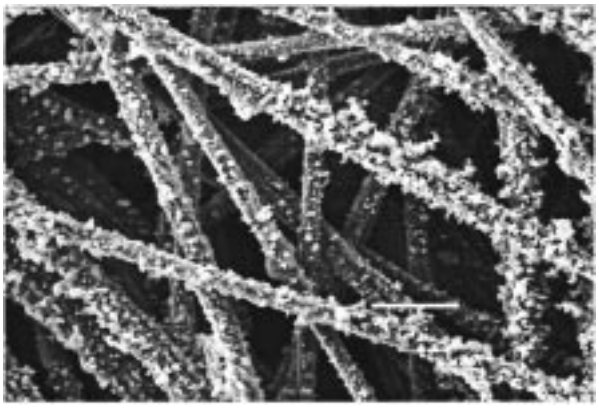

Figure 5. Scanning electron micrograph of the top surface view of a carbon paper electrode after MPFPT was electrodeposited from 0.2 M Et_4NBF_4 in acetonitrile solution (bar = 50 μm).

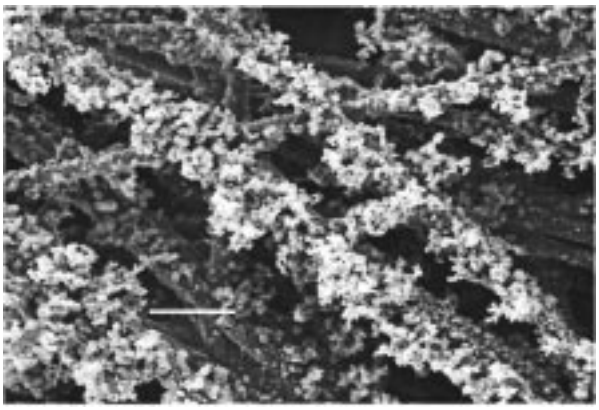

Figure 6. Scanning electron micrograph of the top surface view of a carbon paper electrode after MPFPT was electrodeposited from 0.2 M $Me_4NCF_3SO_3$ in acetonitrile solution (bar = 50 μm).

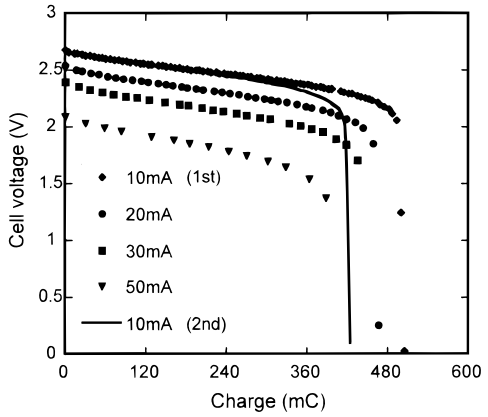

Figure 7. Potential vs discharge curves obtained for a PFPT-based capacitor grown and cycled in 0.2 M $Me_4NCF_3SO_3$ in acetonitrile, recorded at discharge rates of 10, 20, 30, and 50 mA/cm^2 between 2.8 and 1.0 V for 5−10 cycles each, followed by a repeated discharge cycle at 10 mA/cm^2, after charging at a current of 2 mA/cm^2.

morphology control represents a powerful method to influence the performance of the resulting ECC devices.[49]

The total charge collected in discharge at different current densities from a PFPT-based ECC is shown in Figure 7, where the film was grown and cycled in $Me_4NCF_3SO_3$ electrolyte solutions. Figure 8 shows the corresponding data for a film grown and cycled in Et_4NBF_4 electrolyte solutions. The capacitor incorporating the film grown from $Me_4NCF_3SO_3$ has a greater charge density and can deliver this charge at higher rates (Table 3), which we believe is a direct consequence of its more open structure.

(49) Tourillon, G.; Garnier, F. *J. Polym. Sci.* **1984**, *22*, 39.

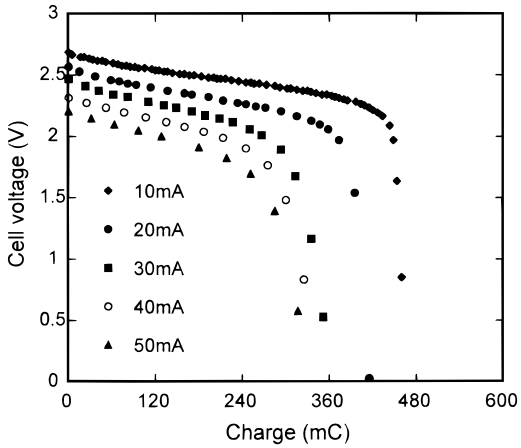

Figure 8. Potential vs discharge curves obtained for a PFPT-based capacitor grown and cycled in 0.2 M Et_4NBF_4 in acetonitrile, recorded at discharge rates of 10, 20, 30, 40, and 50 mA/cm^2 between 2.8 and 1.0 V for 5−10 cycles each, after charging at a current of 2 mA/cm^2.

Table 3. Specific Discharge Values for PFPT Polymer Films Grown and Cycled in 0.2 M $Me_4NCF_3SO_3$ and 0.2 M Et_4NBF_4 Solutions, Respectively

discharge rate (mA/cm^2)	0.2 M $Me_4NCF_3SO_3$[a] (C/g)	0.2 M Et_4NBF_4[b] (C/g)
10	41.7 ± 0.4	40.0 ± 0.4
20	40.0 ± 0.4	35.0 ± 0.4
30	40.0 ± 0.3	28.9 ± 0.4
40	36.7 ± 0.3	28.0 ± 0.4
50	37.5 ± 0.3	22.0 ± 0.4

[a] Films grown from 0.2 M $Me_4NCF_3SO_3$. [b] Films grown from 0.2 M Et_4NBF_4.

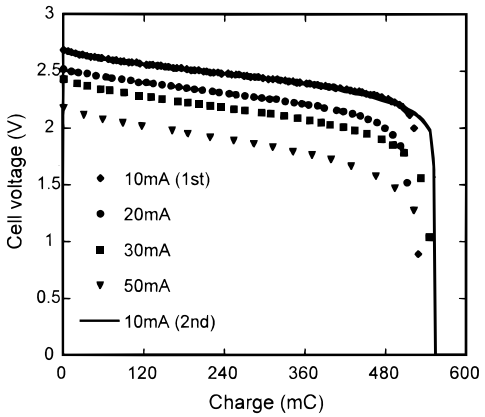

Figure 9. Potential vs discharge curves obtained for an MPFPT-based capacitor grown and cycled in 0.2 M Et_4NBF_4 in acetonitrile, recorded at discharge rates of 10, 20, 30, and 50 mA/cm^2 between 2.8 and 1.0 V for 5−10 cycles each, followed by a repeated discharge cycle at 10 mA/cm^2, after charging at a current of 2 mA/cm^2.

The MPFPT deposits with a nodular structure from both Et_4NBF_4 and $Me_4NCF_3SO_3$ electrolyte solutions (Figures 5 and 6, respectively). The excellent charge dynamics for the MPFPT films grown from these two electrolytes are shown in Figures 9 and 10 and are

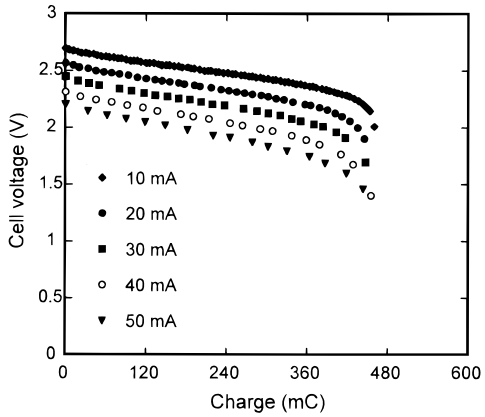

Figure 10. Potential vs discharge curves obtained for an MPFPT-based capacitor grown and cycled in 0.2 M $Me_4NCF_3SO_3$ in acetonitrile, recorded at discharge rates of 10, 20, 30, 40, and 50 mA/cm^2 between 2.8 and 1.0 V for 5−10 cycles each, after charging at a current of 2 mA/cm^2.

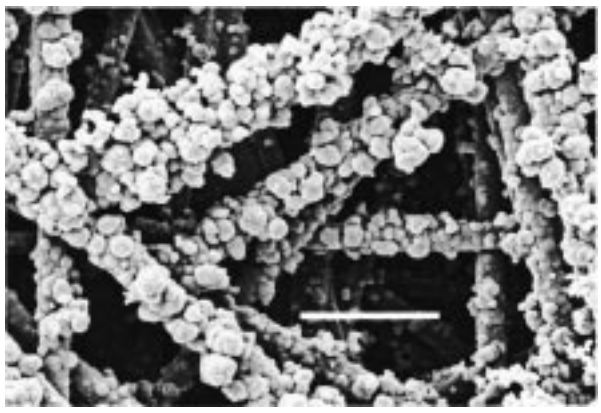

Figure 11. Scanning electron micrograph of the top surface view of a carbon paper electrode after PCNPT was electrodeposited from 0.2 M $Me_4NCF_3SO_3$ in acetonitrile solution (bar = 50 μm).

almost certainly a consequence of their open structures. These figures show that the total charge collected from the MPFPT-based devices at 50 mA/cm^2 is not significantly smaller than that obtained at 10 mA/cm^2.

PCNPT and PMSPT polymer films were both grown from acetonitrile solutions containing 0.1 M monomer and 0.2 M $Me_4NCF_3SO_3$ and their respective morphologies are shown in Figures 11 and 12. Both polymer films exhibited the nodular structure similar to that observed for PFPT and MPFPT grown using this same electrolyte. The preliminary results of the charge/discharge cycles for these two polymers indicate high energy and power densities. Further optimization of these polymer systems is in progress.

Specific Discharge Capacity vs Discharge Rate. The discharge capacities achieved by these devices were

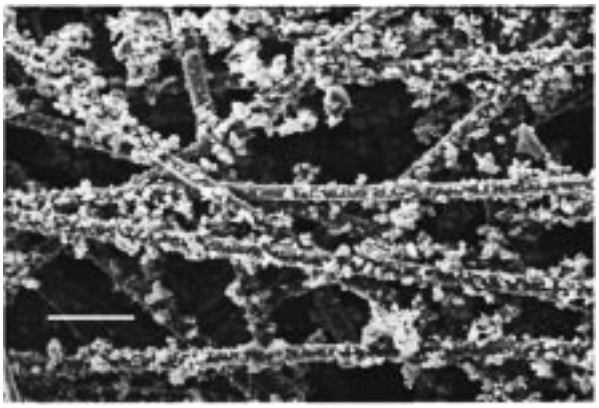

Figure 12. Scanning electron micrograph of the top surface view of a carbon paper electrode after PMSPT was electrodeposited from 0.2 M $Me_4NCF_3SO_3$ in acetonitrile solution (bar = 50 μm).

obtained from discharge experiments recorded at different current densities. The ECCs were repeatedly charged to 2.8 V at 2 mA/cm^2 and discharged at constant currents between 10 and 50 mA/cm^2 in 10 mA/cm^2 steps until the cell voltage reached 1.0 V. For each discharge current, the capacitor was cycled 5−10 times. Finally, it was charged at 2 mA/cm^2 and discharged at 10 mA/cm^2 and these results were compared with the original 10 mA/cm^2 discharge to estimate cycling stability.

ECCs based upon PFPT grown from 0.2 M $Me_4NCF_3SO_3$ were charged and discharged in both 0.2 and 1.0 M $Me_4NCF_3SO_3$. ECCs based upon MPFPT grown from 0.2 M Et_4NBF_4 were charged and discharged in 0.2 and 1.0 M Et_4NBF_4. The specific discharge data (coulombs per gram) for these devices are shown in Table 4. Increasing the concentrations of the electrolyte salts by a factor of 5, and thus the electrolyte conductivity by a factor of 2.5, only affords a less than 10% increase in these values for all the discharge rates.

The discharge curves represented as cell voltage vs discharge capacity are displayed in Figures 7 and 9 for PFPT and MPFPT, respectively. At the lowest discharge current, both the PFPT and MPFPT capacitors show the highest cell voltage and discharge capacities. Upon extended cycling, the discharge capacity (at 10 mA/cm^2) remained essentially unchanged for MPFPT but decreased by 16% for the PFPT-based ECC. The cycle efficiencies (the ratio of the recovered charge/injected charge) for MPFPT capacitors were 96% ± 1%. The corresponding values for PFPT based devices were 90% ± 3%. We believe this difference is again related to the more open structure of MPFPT films compared to the PFPT films. Furthermore, increasing the discharge current from 10 to 50 mA/cm^2 decreases the recovered charge by less than 5% (Figure 14) for this

Table 4. Specific Discharge Values for PFPT-Based ECC Grown from 0.2 M $Me_4NCF_3SO_3$ and for MPFPT-Based ECC Grown from 0.2 M Et_4NBF_4 Solution

	PFPT grown from 0.2 M $Me_4NCF_3SO_3$		MPFPT grown from 0.2 M Et_4NBF_4	
discharge rate (mA/cm^2)	0.2 M $Me_4NCF_3SO_3$ (C/g)	1.0 M $Me_4NCF_3SO_3$ (C/g)	0.2 M Et_4NBF_4 (C/g)	1.0 M Et_4NBF_4 (C/g)
10	41.7 ± 0.4	45.0 ± 0.5	54.0 ± 0.1	58.9 ± 0.3
20	40.0 ± 0.4	41.7 ± 0.6	53.5 ± 0.3	57.4 ± 0.1
30	40.0 ± 0.3	42.3 ± 0.1	56.4 ± 0.3	57.9 ± 0.1
40	36.7 ± 0.3	41.3 ± 0.4	54.5 ± 0.4	56.9 ± 0.3
50	37.5 ± 0.3	40.0 ± 0.1	55.4 ± 0.4	56.4 ± 0.3

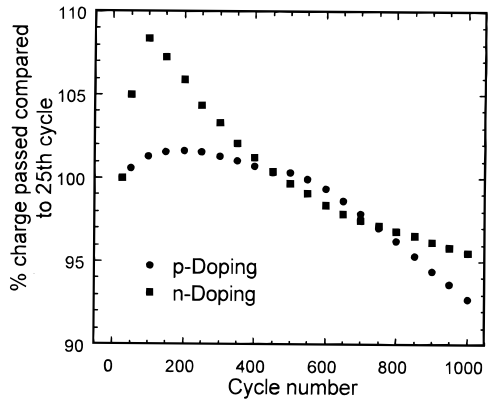

Figure 13. Percentage charge passed compared to the 25th cycle vs cycle number for MPFPT films electropolymerized from 0.2 M Et_4NBF_4 onto carbon paper at 1.5 mA/cm^2 current density for 4500 s and cycled between −1.4 and −2.15 V vs Ag/Ag$^+$ and 0 and 1 V vs Ag/Ag$^+$, respectively, at 50 mV s^{-1} in 0.2 M Et_4NBF_4.

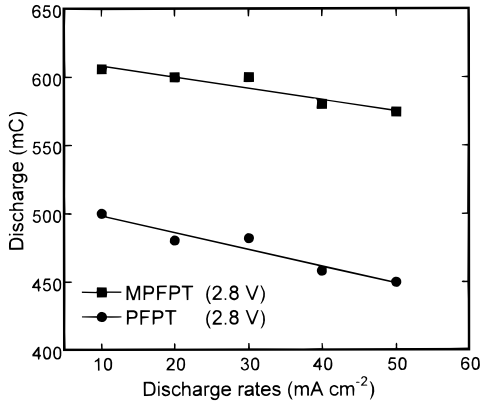

Figure 14. Discharge values vs discharge rates for MPFPT- and PFPT-based capacitors grown and cycled in 0.2 M Et_4NBF_4 and in 0.2 M $Me_4NCF_3SO_3$, respectively.

system, whereas comparable values for the PFPT device are in the 10−20% range.

Cyclability and Stability. The degradation of the PFPT and MPFPT polymer films deposited on either a Pt electrode or carbon paper was evaluated using cyclic voltammetry on single electrodes. Table 5 summarizes the data collected for the Pt electrodes. It can be seen that both PFPT and MPFPT show very little degradation in the p-doping regime under these conditions. In the n-doping region PFPT shows considerable degradation but MPFPT has a stability even better than that seen in the p-doping region. This result led us to test the stability of MPFPT deposited onto the carbon substrates. Figure 13 shows the percentage of the total charge [(inserted charge + extracted charge)/2], compared to the amount passed on the 25th cycle, vs cycle number as recorded via cyclic voltammetry between −1.4 and −2.15 V (n-doping) and 0.0 and 1.0 V (p-doping) vs Ag/Ag$^+$ at a scan rate of 50 mV s^{-1}. The behavior of the films deposited on C is different from that seen on the Pt electrode. In the n-doping region there is a significant increase in the charge passed between the 25th and the 100th cycles (similar growth was also observed for cycles 1−25) whereas the portion of the curve between the 100th and the 1000th cycle shows exponential decay. It is interesting to note that during the initial 100 cycles the charge balance (extracted charge/inserted charge) for the individual voltammograms increased from approximately 80% to 98% with cycle number and then remained constant for the remainder of the experiment. This indicates that there is no kinetic limitation for the extraction process after the initial 100 cycles. This suggests that the initial cycles act as a conditioning period, which is associated with an opening of the polymer structure on the microscopic scale along with a swelling of the material due to solvent and salt retention. The subsequent loss of charge may be due to either slow degradation of the polymer or a loss of polymer in electrical contact with the C substrate. This loss of contact could result from the repeated swelling and contraction of the polymer film during the doping and dedoping processes. For the p-doping region an initial increase in the amount of charge passed was also observed (cycles 1−150), but the increase is not as dramatic as that observed for the n-doping process. This behavior may be ascribed to a similar conditioning process. However, the amount of charge passed during the period 150−500 decreases by a small amount and an almost linear fall in the amount of charge is observed on continued cycling (cycles 500−1000). This would seem to indicate that a parasitic reaction is occurring during cycling and that it is consuming the polymer at a steady rate or that during potentiodynamic cycling of this type the amount of polymer that is electrochemically active decreases at a steady rate. This implies that the degradation mechanisms may differ for the p- and n-doping regimes. Further work is in progress to clarify these issues.

Even though MPFPT retains >90% of its maximum charge in both the p- and n-doping regimes over 1000 cycles in the present configuration, we expect this can be further extended by even more careful attention to issues such as solvent and electrolyte dryness and purity.

Energy and Power Densities. The Ragone plots for our ECCs are shown in Figures 15 and 16. The energy densities were calculated from the discharge capacity, the deposited polymer mass, and the actual cell voltage, and the power density was calculated by dividing the energy density by the discharge time. The reported values are *for electroactive polymer only* and are an average of three devices.

Table 5. Degradation Percentage of the p- and n-Dedoping Charges after 100 Cycles for MPFPT and PFPT Grown on Pt Electrodes

polymer	growth electrolyte[a]	growth current density (mA/cm^2)	cycling electrolyte 100 cycles	degradation % n-dedoping	degradation % p-dedoping
PFPT	0.2 M $Me_4NCF_3SO_3$	11	$Me_4NCF_3SO_3$	21	3
PFPT	0.2 M $Me_4NCF_3SO_3$	3	$Me_4NCF_3SO_3$	18	2
MPFPT	0.2 M Et_4NBF_4	11	Et_4NBF_4	<1	2
MPFPT	0.2 M Et_4NBF_4	3	Et_4NBF_4	0	<2

[a] In each case a Pt electrode was used.

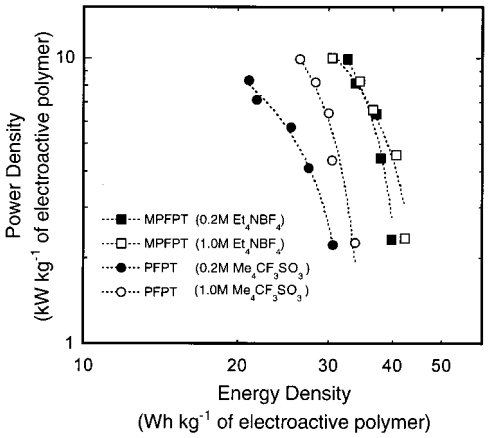

Figure 15. Ragone plot for PFPT-based capacitors grown from 0.2 M $Me_4NCF_3SO_3$ and cycled in 0.2 M $Me_4NSCF_3SO_3$ and 1.0 M $Me_4NCF_3SO_3$ and MPFPT-based capacitors grown from 0.2 M Et_4NBF_4 and cycled in 0.2 M Et_4NBF_4 and 1.0 M Et_4NBF_4. The capacitors were charged to 2.8 V at 2 mA/cm^2 and discharged at current densities of 10−50 mA/cm^2.

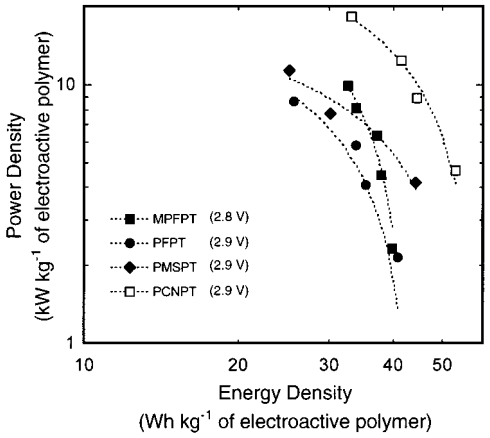

Figure 16. Ragone plot of a MPFPT-based capacitor grown and cycled in 0.2 M Et_4NBF_4 and discharged from 2.8 V and PFPT-, PCNPT-, and PMSPT-based capacitors grown and cycled in 0.2 M $Me_4NCF_3SO_3$ and discharged from 2.9 V. All capacitors were charged at 2 mA/cm^2.

The highest performance PFPT-based capacitors utilized polymers grown and cycled in $Me_4NCF_3SO_3$. Upon increasing the electrolyte concentration from 0.2 to 1.0 M, both the energy and power densities are enhanced (9−17% and 2−16% increases, respectively) for the PFPT-based ECC (Figure 15). The devices exhibited energy densities of 40.5 ± 1.3 Wh/kg (based on electroactive polymer) and power densities of 2.2 ± 0.25 kW/kg (electroactive polymer) for a cell voltage of 2.9 V and a discharge current of 10 mA/cm^2. Comparable performance was achieved for MPFPT-based devices charged to only 2.8 V (40 ± 1 Wh/kg, 2.6 ± 0.3 kW/kg). When a discharge current of 50 mA/cm^2 was demanded from the MPFPT-based capacitors, these values were 32.7 ± 1.5 Wh/kg and 10.7 ± 0.7 kW/kg (Figure 15). Considerably smaller increases in energy and power densities were observed for MPFPT in going from 0.2 to 1.0 M electrolyte, compared to PFPT devices.

Energy (power) densities of 53 ± 3 Wh/kg (4.6 ± 0.7 kW/kg) and 44.3 ± 3.5 Wh/kg (4.2 ± 0.5 kW/kg) were obtained for PCNPT and PMSPT-based ECCs, respectively, discharged from 2.9 V at 10 mA/cm^2 (Figure 16). The values for PCNPT are among the highest reported for any polymer at this discharge rate and cell voltage, and detailed studies on this system will be the subject of a future report.

Conclusions

By careful choice of the growth conditions and the electrolyte salt and concentration, films with optimized morphologies were produced. Once deposited, enhanced charge capacity and cyclability were realized by an equally careful choice of the electrolyte solution in the device. However, the selection of growth and device electrolytes were monomer/polymer-dependent.

The specific discharge capacities obtained in these studies are among the highest reported for polymer-based electrochemical capacitors. The MPFPT-based capacitor is particularly promising in that it displays high capacity and superior charge/discharge performance. MPFPT showed virtually no degradation for the p- and n-doping processes on the Pt electrode. On extended cycling on C electrodes, a small but steady decrease in the charge was observed after an initial increase in both the p- and n-doping regions. However, the performance of the electrodes was still satisfactory after 1000 cycles. The longer term stability of these materials is presently being investigated. Preliminary results for PCNPT-based devices suggest that type III electrochemical capacitors using this polymer may even exceed MPFPT's performance.

Acknowledgment. This work was supported by HECB of the state of Texas and Los Alamos National Laboratories. We also thank Andrew Moxey for providing the electrolyte conductivity data and for his valuable discussions.

CM9803105